Experimental Mechanics
DOI 10.1007/s11340-012-9710-5

Nonlinear Acoustic Interaction of Contact Interfaces

J.-P. Jiao · W-H. Liu · C-F. He · B. Wu · J. Zhang

Received: 7 May 2012 / Accepted: 20 December 2012

Abstract Nonlinear acoustic interactions at contact interfaces can be used to characterize defects or imperfect bonds at these interfaces. Most methods used to characterize nonlinear interactions consider only a portion of the nonlinear signature, such as nonlinearities caused by high-order harmonics or sidebands. We describe a signal processing algorithm that can extract three nonlinear indicators related to amplitude attenuation, phase shift, and harmonics. Two aluminum blocks were mounted together to form a contact interface and subjected to normal compressive loading. Experiments were conducted to investigate the nonlinear interactions between the ultrasonic waves and interfaces, with a focus on the influence of excitation levels, applied pressure, and surface roughness. The ultrasonic signals were then processed using the nonlinear feature extraction algorithm. We show that the nonlinear indicators can characterize the contact condition of interfaces, and that their sensitivities to pressure differ for interfaces of different roughness and over different pressure ranges.

Keywords Nonlinear acoustics · Interfaces · Amplitude attenuation · Phase shift · Harmonics

Introduction

The transmission and reflection characteristics of ultrasonic waves at contact surfaces have been extensively studied to evaluate bonded interfaces and for tribological monitoring [1, 2]. When an ultrasonic wave with sufficiently high amplitude is incident on such surfaces, repeated collisions are generated between the two surfaces. These repeated interactions result in nonlinear acoustic responses, known as contact acoustic nonlinearities (CANs). CANs have attracted increasing attention and have been used to characterize defects and imperfect bonding at interfaces [3, 4].

We assume that the relationship between the input ultrasonic waves and the output response is initially linear. When linearity is violated, the input and output are not compatible in terms of their frequency components. Possible reasons for an observed nonlinear acoustic response are that: (1) The wave speed is dependent on the elastic constant of the material which causes the phase shift in the recorded signal; (2) The amplitude of the recorded signal is influenced by nonlinear attenuation; (3) Nonlinear coupling allows the generation of high-order harmonics, sidebands, or subharmonics, which are generally used to indicate the presence of nonlinear scattering in samples.

Although defects and imperfections can be detected by high-order harmonics [5, 6], subharmonics [7, 8], and sidebands [9, 10] extracted from the nonlinear acoustic response, these approaches do not always work satisfactorily in practice. A major cause of invalidity of these indicators is the difficulty in distinguishing the nonlinearity from the generation/acquisition system and the defects. Extracting perceptible features which allow early damage detection is also challenging [11, 12]. High-order harmonics, subharmonics, and sidebands only represent part of the nonlinear signature. The contribution of the fundamental frequency has until now been neglected because of amplitude attenuation and phase shift, which are also sensitive to nonlinear scattering [13, 14].

To better evaluate the acoustic nonlinearities at a compressed interface, the present work aims to develop a method that can extract all possible nonlinear components.

Fundamental Theory

The acoustic response of an elastic medium to an elastic wave with amplitude A and angular frequency ω_0, which

J.-P. Jiao (✉) · W.-H. Liu · C.-F. He · B. Wu
Department of Mechanical Engineering, Beijing University of Technology, Beijing 100124, China
e-mail: jiaojp@bjut.edu.cn

W.-H. Liu
BAIC Motor Electric Vehicle Co., Ltd, Beijing 102606, China

J. Zhang
Department of Mechanical Engineering, University of Bristol, Bristol, UK

Published online: 09 January 2013

can be expressed as the superposition of simple harmonic waves [13, 14]:

$$v_A(t) = \sum_{n=1}^{\infty} B_n(A)\cos[n\omega_0 t + \varphi_n(A)] \tag{1}$$

where $v_A(t)$ is the acoustic response, and $B_n(A)$ and $\varphi_n(A)$ are the amplitude and phase of the harmonic waves, respectively. These values are functions of the amplitude A.

When the sample is excited at sufficiently low amplitude, A_{lin}, the strain is small, and the nonlinear contributions from the stress–strain relationship are negligible. As a result, the recorded signals do not contain high-order harmonics, but only the following fundamental component:

$$v_{lin}(t) = B_1(A_{lin} \to 0)\cos(\omega_0 t + \varphi_0) \tag{2}$$

We assume that $\varphi_0 = 0$ and define a reference signal with an arbitrary, finite amplitude A $[A = kA_{lin}(k >> 1)]$:

$$v_{ref}(t) = kv_{lin}(t) = kB_1(A_{lin})\cos(\omega_0 t) \neq v_A(t) \tag{3}$$

When the sample is excited with a sufficiently large amplitude (referred to as the finite amplitude excitation), the nonlinear contributions occur in the elastic response, and the higher harmonics in equation (1) cannot be ignored. As a result, the nonlinear components can be defined by the difference between the harmonic response to the finite amplitude excitation and the corresponding reference signal:

$$w_A(t) = v_A(t) - v_{ref}(t) \tag{4}$$

Combining equations (1) and (3), the nonlinear components w_A can be expressed as

$$\begin{aligned} w_A(t) = {} & -kB_1(A_{lin})\cos(\omega_0 t) + B_1(A)\cos[\omega_0 t + \varphi_1(A)] \\ & + \sum_{n=2}^{\infty} B_n(A)\cos[n\omega_0 t + \varphi_n(A)] \end{aligned} \tag{5}$$

To separate the nonlinear components, the polynomial k $B_1(A_{lin})\cos[\omega_0 t + \varphi_1(A)]$ is introduced. Equation (5) can then be rewritten as

$$\begin{aligned} w_A(t) = {} & kB_1(A_{lin})\cos[\omega_0 t + \varphi_1(A)] - kB_1(A_{lin})\cos(\omega_0 t) \\ & + B_1(A)\cos[\omega_0 t + \varphi_1(A)] - kB_1(A_{lin})\cos[\omega_0 t + \varphi_1(A)] \\ & + \sum_{n=2}^{\infty} B_n(A)\cos[n\omega_0 t + \varphi_n(A)] \end{aligned} \tag{6}$$

In equation (6), the first two terms can be regarded as the nonlinear contribution caused by the phase shift. The last term is the nonlinear contribution from the harmonics, and the other two terms can be considered as the nonlinear contribution due to amplitude attenuation. Hence, the nonlinear components in the elastic response can be rewritten as

$$w_A(t) = w_1(t) + w_2(t) + w_3(t) \tag{7}$$

where $w_1(t)$ is the phase nonlinearity:

$$w_1(t) = -2kB_1(A_{lin})\sin\left(\omega_0 t + \frac{\varphi_1(A)}{2}\right)\sin\left(\frac{\varphi_1(A)}{2}\right) \tag{8}$$

$w_2(t)$ is the attenuation nonlinearity:

$$w_2(t) = [B_1(A) - kB_1(A_{lin})]\cos[\omega_0 t + \{\varphi_1(A)] \tag{9}$$

and $w_3(t)$ the harmonic nonlinearity:

$$w_3(t) = \sum_{n=2}^{\infty} B_n(A)\cos[n\omega_0 t + \varphi_n(A)] \tag{10}$$

An indicator, $\theta(A)$, is defined to quantify the nonlinear contributions:

$$\theta(A) = \frac{1}{nT}\int_0^{nT} w_A^2(t)dt \tag{11}$$

where $\theta(A)$ is a nonlinear indicator, n is a positive integer, and T is the period of the signal.

For phase nonlinearity, the corresponding phase indicator is as follows:

$$\theta_1(A) = 2k^2 B_1^2(A_{lin})\sin^2\left(\frac{\varphi_1(A)}{2}\right) \tag{12}$$

The attenuation indicator is defined as

$$\theta_2(A) = \frac{1}{2}[B_1(A) - kB_1(A_{lin})]^2 \tag{13}$$

Experimental System and Signal Procedure

The experimental setup for the ultrasonic evaluation of the interfaces is shown in Fig. 1. Two 30-mm-high and 30-mm-wide aluminum blocks were mounted and pressed against each other in a loading frame. The contact interface was subjected to a loading–unloading cycle of up to 75 kN, and the compressive load was measured using a load cell. The transmitted acoustic waves were measured at different pressure levels. Four types of samples with different surface roughness were prepared. The average root mean square roughness values of the sample surfaces used were 0.4, 0.8, 1.6, and 3.2 μm.

A sinusoidal tone burst with 30 periods and 5 MHz central frequency was generated using a function generator. The tone burst was amplified using a power amplifier, filtered by a low-pass filter, and then applied to a longitudinal transducer with a 5 MHz nominal frequency to excite longitudinal waves at the

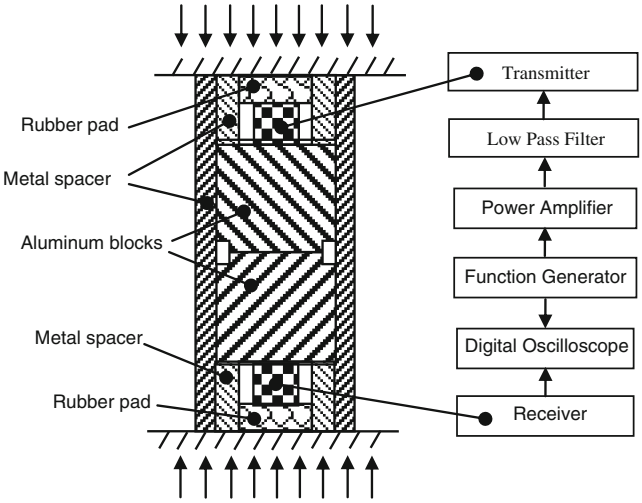

Fig. 1 Schematic diagram of the experimental setup

interface. The transmitted acoustic waves were detected using a wideband transducer with a 10 MHz central frequency. The transmitter and receiver were coupled to the aluminum blocks using glycerin as the coupling medium. To maintain a constant coupling force, rubber pads were used as shown in Fig. 1. The output voltage of the function generator was varied from 100 to 300 mV with a step size of 20 mV. The transmitted waveforms were captured with a digital oscilloscope. Prior to the measurements, the contact interface was subjected to several loading–unloading cycles to avoid significant hysteresis caused by inelastic flattening during the first loading stage.

To extract the individual nonlinear components, the detected signal $v_A(t)$ was processed in three different ways as described below and shown in Fig. 2.

1) Phase nonlinearity: The original signal $v_A(t)$ was filtered around the fundamental frequency (band-pass filter, $0.5\,\omega_0 < \omega$). The result was normalized to the amplitude of the reference signal $\left[v_{ref}(t) = kB_1(A_{lin})\cos(\omega_0 t)\right]$. Assuming that the experimental signals approximately correspond to those theoretically expected from equations (1) and (2), $v_A'(t) = kB_1(A_{lin})\cos[\omega_0 t + \varphi(A)]$; therefore, $w_1(t) = v_A'(t) - v_{ref}(t)$. The phase indicator was obtained from equation (12).
2) Attenuation nonlinearity. The original signal $v_A(t)$ was filtered around the fundamental frequency (band-pass filter, $0.5\omega_0 < \omega$). The reference signal was phased-shifted with respect to the measured signal, i.e., $v_{ref}(t)$ was shifted in time to obtain maximum correlation with $v_A(t)$. The experimental signals were assumed to approximate the theoretically expected values obtained from equation (2). Accordingly, the shift corresponding to a maximum correlation is $t = \phi_1(A)/\omega_0$ and $v_A''(t) = B(A)\cos[\omega_0(t-t) + \phi_1(A)] = B(A)\cos(\omega_0 t)$; therefore, $w_2(t) = v_A''(t) - v_{ref}(t)$. The attenuation indicator was obtained from equation (13).
3) Harmonic nonlinearity: The original signal $v_A(t)$ was high-pass filtered $(1.5\omega_0 < \omega$ and $v_A^F(t)$ was obtained. Thus, in this case, $w_3(t) = v_A^F(t)$.

Results and Discussion

Ultrasonic experiments were conducted for samples at different excitation levels at each loading step. Typical waveforms obtained at the different excitation levels (i.e., 220, 240, 260, 280, and 300 mV) for an applied pressure of 10 kN are illustrated in Fig. 3. With an increase in excitation level, the amplitude of the received signal gradually increased, with the signal becoming distorted both in amplitude and phase after transmitting through the interface under pressure. However, directly illustrating the variations in amplitude and phase through the waveforms is difficult.

Nonlinearity Representation at Different Pressure Levels

To extract the individual nonlinear components, the detected signals were processed using the algorithm shown in Fig. 2. The total nonlinear component and three nonlinear indicators are shown in Fig. 4 as a function of contact pressure at different excitation levels. The total nonlinear component, phase indicator, attenuation, and harmonics indicators are represented in Fig. 4(a)–(d), respectively. The surfaces

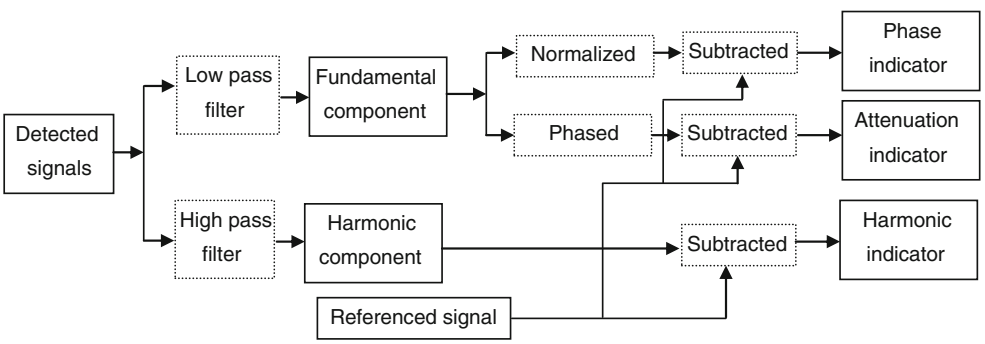

Fig. 2 Flow chart of the signal analysis for the nonlinear indicator extraction

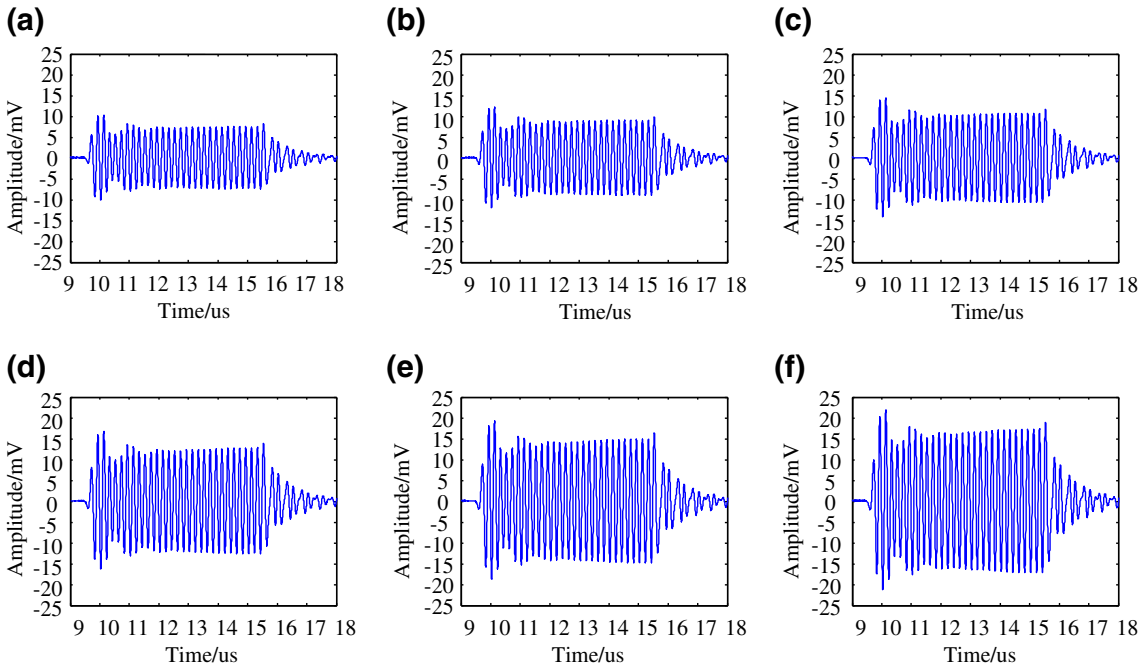

Fig. 3 Typical waveforms received at different excitation levels for an applied pressure of 10 kN: (**a**) 200, (**b**) 220, (**c**) 240, (**d**) 260, (**e**) 280, and (**f**) 300 mV

forming the interface had the same roughness (0.4 μm). The total nonlinear component varied with the applied pressure. The variation tendencies of the three individual indicators and their sensitivities to pressure differed drastically, depending strongly on the pressure range. However, the indicators exhibited similar behavior at different excitation levels. Based

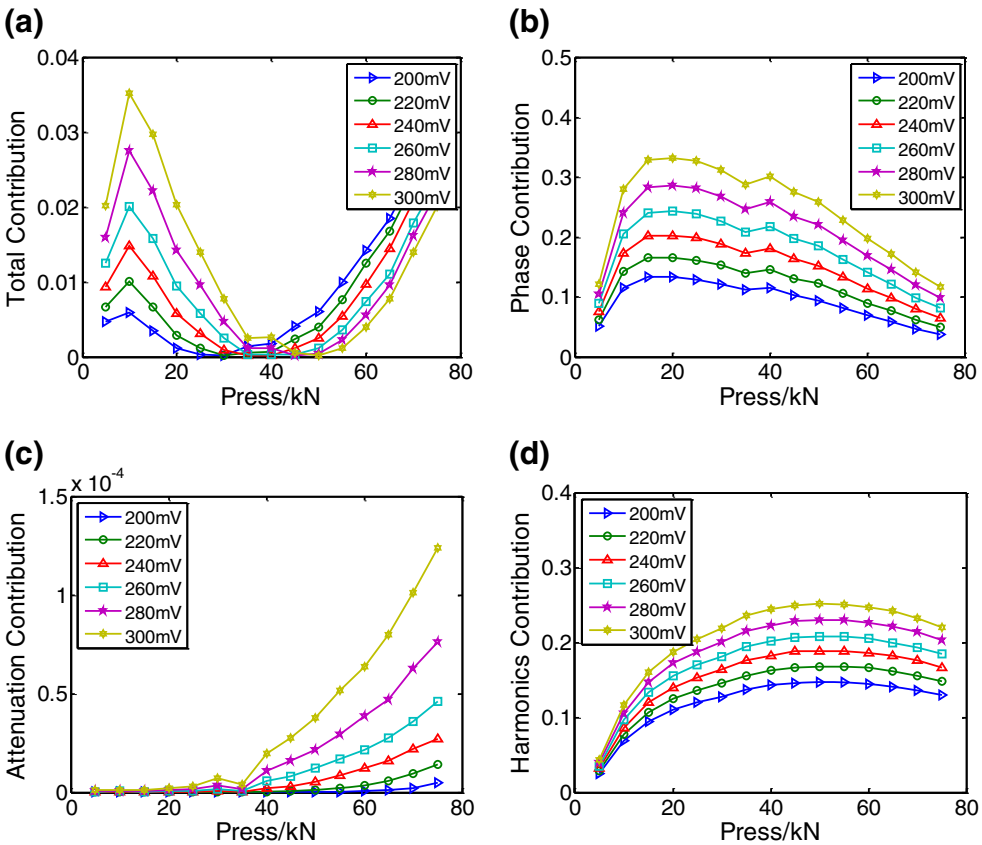

Fig. 4 Nonlinear components as a function of contact pressure at different excitation amplitudes. (**a**) Total component, (**b**) phase indicator, (**c**) attenuation indicator, and (**d**) harmonics indicator

on the variation tendency of the three indicators, the contact condition of the interfaces can be evaluated in three discrete ranges, 5 to 15 kN, 15 to 40 kN, and 40 to 75 kN.

In the first pressure range (5 to 15 kN), the phase indicator was most sensitive to pressure, with direct proportionality observed, as shown in Fig. 4(b). The attenuation indicator was insensitive to pressure when the pressure was less than 40 kN, as shown in Fig. 4(c), and the harmonics indicator slowly increased with pressure, as shown in Fig. 4(d). This behavior is possibly caused by the change in the contact condition at the interface as a result of the collapse of interfacial microstructures, which would lead to a temporary increase in the interfacial stiffness and bulk modulus, thereby resulting in a phase shift in the recorded signals.

In the second pressure range (15 to 40 kN), the phase and attenuation indicators were approximately constant, whereas the harmonics indicator slightly increased with increasing pressure. In this range, the deformation of the interface can be considered quasilinear elastic and no significant changes in the interfacial stiffness were observed.

In the third pressure range (40 to 75 kN), the attenuation indicator was the most sensitive parameter to pressure. The phase indicator also varied discernibly within this pressure range, however, the harmonics indicator was approximately constant. At high-load levels, the elastoplastic behavior of the interfaces during the loading process cannot be neglected. With increasing pressure, the interfacial stiffness gradually began to decrease, which is related to a decrease in the bulk modulus because of the progression of damage caused by the load.

Therefore, the nonlinear indicators were sensitive in the regime where the interfacial stiffness exhibited variation, most likely because of microstructure collapse or elastoplastic behavior at the surfaces.

Influence of Roughness on Contact Nonlinearity

In this section, the influence of surface roughness on the contact condition of the pressed interface is experimentally investigated. The contact interface was formed by two aluminum blocks of different roughness. The roughness of the bottom block was 0.4 μm, whereas the upper block had varied roughness of 0.8, 1.6, and 3.2 μm. The amplitude of the excited signal was 280 mV.

The variation of the nonlinear indicators as a function of applied pressure for interfaces of different roughness is shown in Fig. 5. The total nonlinear component varied with pressure. At low pressure (below 40 kN), the phase indicator was particularly sensitive to pressure. In contrast, the variations in the attenuation and harmonics indicators were quite small and almost independent of pressure. This behavior was the same for all

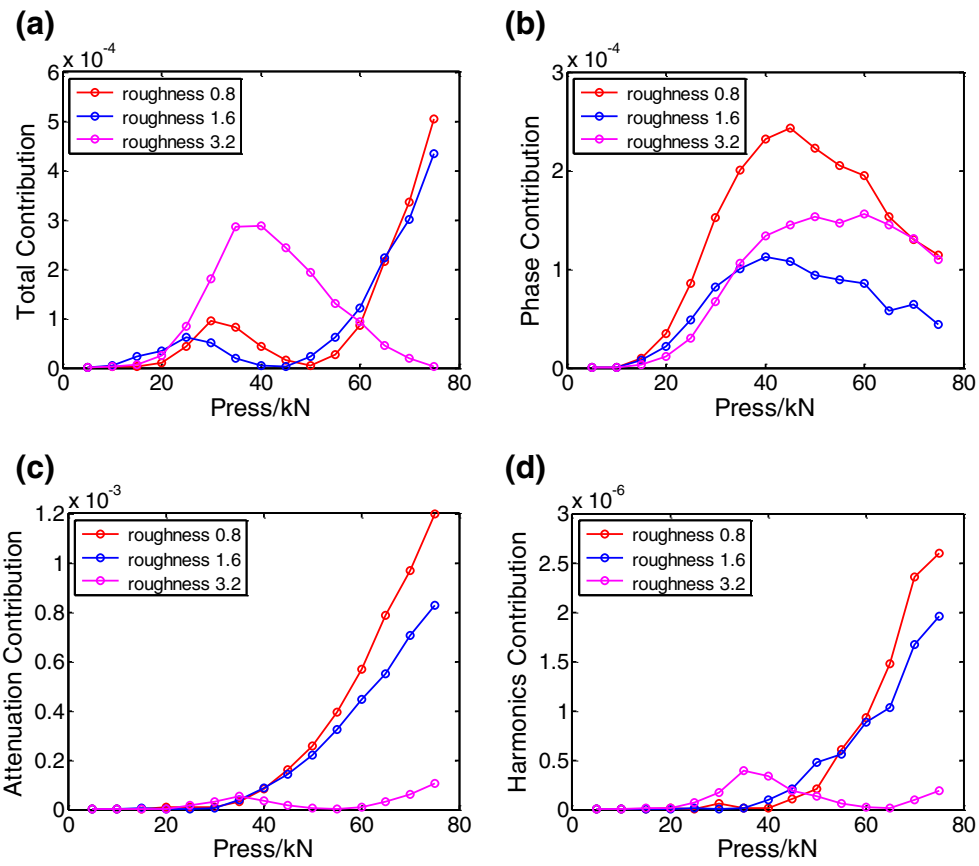

Fig. 5 Nonlinear components as function of applied pressure for interfaces of different roughness. (**a**) Total components, (**b**) phase indicator, (**c**) attenuation indicator, and (**d**) harmonics indicator

levels of roughness and can be attributed to changes at the interface, which increase stiffness, resulting in a phase shift in the recorded signal.

At high pressure (above 40 kN), the attenuation and harmonics indicators were sensitive to pressure for interfaces with low values of roughness (0.8 μm and 1.6 μm). For rough interfaces (3.2 μm), the attenuation and harmonics indicators were not sensitive to pressure. The phase indicator decreased with increasing pressure for all interfaces, reinforcing that elastoplastic deformation cannot be neglected at high pressure.

The experimental conditions, such as the relative position and mounting method of the samples, considerably influenced the initial contact condition of the interfaces, thereby affecting the experimental results. Therefore, in Figs. 4 and 5, the variation tendencies of the three indicators exhibited a certain degree of inconsistency. Nevertheless, the nonlinear indicators can still be used to characterize the contact condition of interfaces within a limited pressure range (at either low or high pressure).

Conclusion

Considering the multiple origins of nonlinearity, a signal processing algorithm was developed to extract the nonlinear components in an acoustic response. Three nonlinear indicators, namely, amplitude attenuation, phase shift, and harmonics, were proposed to evaluate the contact condition of interfaces under applied pressure. A series of experiments were conducted under different conditions to investigate the influence of excitation level, applied pressure, and surface roughness. The three nonlinear indicators were able to characterize the contact condition of the interfaces studied, but their sensitivities to pressure change differed significantly depending on the surface roughness and applied pressure range. At low pressure, the phase indicator was the most sensitive parameter to pressure. At high pressure, the attenuation and harmonics indicators were sensitive to pressure for interfaces of low roughness. However, the phase indicator was sensitive to pressure for rough interfaces. Thus, the proposed nonlinear indicators can provide information on the contact condition of interfaces and a wide understanding of the mechanisms responsible for nonlinear interactions of acoustic waves at interfaces.

Acknowledgments This work was supported by the National Natural Science Foundation of China (grant nos. 51075012 and 11272017) and the Beijing Natural Science Foundation (grant no. 1122005).

References

1. Dwyer-Joyce RS (2005) The application of ultrasonic NDT techniques in tribology. J Eng Tribol 219(5):347–366
2. Anderson WB (2001) Development of a condition monitoring system for mechanical seals. Dissertation, Georgia Institute of Technology
3. Jhang KY (2009) Nonlinear ultrasonic techniques for nondestructive assessment of micro damage in material: a review. Int J Precis Eng Manuf 10(1):123–135
4. Van Den Abeele KE-A, Carmeliet J, Ten Cate JA, Johnson PA (2000) Nonlinear elastic wave spectroscopy (NEWS) techniques to discern material damage, Part II: Single-mode nonlinear resonance acoustic spectroscopy. Res Nondestruct Eval 12(1):31–42
5. Baltazar A, Rokhlin SI, Pecorari C (2002) On the relationship between ultrasonic and micromechanical properties of contacting rough surfaces. J Mech Phys Solids 50(7):1397–1416
6. Drinkwater BW, Dwyer-Joyce RS, Cawley P (1996) A study of the interaction between ultrasound and a partially contacting solid-solid interface. Proc R Soc London 452(1955):2613–2628
7. Abdel-Rahman EM, Nayfeh AH (2005) Contact force identification using the subharmonic resonance of a contact-mode atomic force microscopy. Nanotechnology 16(2):199–207
8. Ohara Y, Yamamoto S, Mihara T, Yamanaka K (2008) Ultrasonic evaluation of closed cracks using subharmonic phased array. Jpn J Appl Phys 47(5):3908–3915
9. Donskov D, Sutin A (1998) Vibro-acoustic modulation nondestructive evaluation technique. J Intell Mater Syst Struct 9:766–771
10. Kim JY, Yakovlev VA, Rokhlin SI (2004) Surface acoustic wave modulation on a partially closed fatigue crack. J Acoust Soc Am 115(5):1961–1971
11. Buck O, Morris WL, Richardson JM (1978) Acoustic harmonic generation at unbonded interfaces and fatigue cracks. Appl Phys Lett 33(5):371–373
12. Biwa S, Nakajima S, Ohno N (2004) On the acoustic nonlinearity of solid-solid contact with pressure-dependent interface stiffness. J Appl Mech 71(4):508–515
13. Bruno CLE, Gliozzi AS, Scalerandi M, Antonaci P (2009) Analysis of elastic nonlinearity using the scaling subtraction method. Phys Rev B 79:064108
14. Scalerandi M, Gliozzi AS, Bruno CLE, Masera D, Bocca P (2008) A scaling method to enhance detection of a nonlinear elastic response. Appl Phys Lett 92:101912